# Photoemission Energy Distributions for Au from 10 to 40 eV Using Synchrotron Radiation*

D. E. Eastman and W. D. Grobman
*IBM Thomas J. Watson Research Center, Yorktown Heights, New York 10598*
(Received 29 March 1972)

High-resolution (typically 0.15 eV) electron energy distributions are reported for Au at closely spaced intervals of photon energy in the 10- to 40-eV range. The data show much $d$-band structure which continuously varies in energy position and amplitude as the photon energy is varied, thereby indicating conservation of crystal momentum over the entire measured range. An experimental density of states for Au has been determined from the data by averaging over all photon energies using a modified $f$-sum rule for photoemission.

Synchrotron radiation from a storage ring provides an ultrahigh vacuum source of intense linearly polarized continuum radiation from the infrared into the x-ray region.[1] While synchrotron radiation has been used extensively in vacuum ultraviolet and soft-x-ray optical absorption and reflection measurements of solids, it has enjoyed very limited use in photoemission measurements of solids. Previously, only photoemission quantum-yield measurements have been reported.[2,3] We present high-resolution (typically 0.15 eV) energy distribution curves (EDC's) for Au which were obtained in the photon energy range $10 \lesssim h\nu \lesssim 40$ eV. Synchrotron radiation from the 240-MeV storage ring at the University of Wisconsin Physical Sciences Laboratory was used together with a windowless photoelectron spectrometer having a two-stage cylindrical-mirror electron analyzer. Our data greatly extend the normal range of photon energies $h\nu$, which is typically limited to continuous energies below 11.6 eV (LiF-window cutoff) plus several resonance lines (16.8, 21.2, 26.9, and 40.8 eV).[4-6]

Our photoemission spectra for Au show much structure which varies in energy position and amplitude as a result of momentum conservation as $h\nu$ is continuously varied in the 10–40-eV range. These data should provide a detailed test of one-electron band theory over this wide range of energy. Comparison of theory and experiment should also be faciliated by the availability of experimental EDC's at all $h\nu$'s, since trends and thresholds for various elements of structure can be obtained. Theoretical calculations of photoemission spectra based on one-electron band calculations with momentum-conserving interband optical excitations have been reported for Au for $h\nu \leq 11.6$ eV.[6,7] Similar calculations for Cu, which include interband momentum matrix elements, have been recently reported[8] for energies up to $h\nu \simeq 30$ eV, and such calculations can be made for Au over our measured energy range.

We have determined an experimental valence-band density of states for Au by averaging our data using a modified $f$-sum rule. This density of states for Au shows a close similarity to the x-ray photoelectron spectra for Au reported by Shirley,[9] and to theoretical densities of states for Au determined from relativistic energy-band calculations.[6,7]

Characteristics of synchrotron radiation from the 240-MeV storage ring at the University of Wisconsin Physical Sciences Laboratory have been described.[1] We have constructed a windowless photoelectron spectrometer which consists of a retard/accelerate stage constructed from two concentric hemispherical grids (each 82% transparent) centered about the sample, followed by a two-stage electrostatic deflection, cylindrical-mirror electron analyzer[10] and a Bendix channeltron electron multiplier.

A two-stage cylindrical-mirror analyzer simplifies sample alignment and minimizes effects due to stray light and secondary electron emission. That is, only electrons originating from a small spherical spatial region $\sim 1$ mm$^3$ can pass through both stages. The passband width $\Delta E$ is determined by selecting the pass energy $E$, where the calculated resolution of the analyzer is $R = \Delta E/E \simeq 0.6\%$.

We used a 1-m normal-incidence vacuum monochromator with a 1200 1/mm Au-coated grating constructed by the Physical Sciences Laboratory. The exit-slit assembly of the monochromator was removed and our photoelectron spectrometer was placed so that the sample was located at the monochromator exit-slit position. This eliminates the need to focus the exit slit on the sample and simplifies optical alignment of the system.

Au films of 1000–5000 Å thickness were prepared by evaporation onto an air-cleaved $\langle 111 \rangle$ Si substrate of area 4 mm$^2$ using a filament bead

evaporator. During operation, the pressure was in the $10^{-8}$-Torr range in the monochromator and was about $3\times10^{-10}$ Torr in the spectrometer. During evaporation, at rates of roughly 3–20 Å/sec, the pressure rose into the $10^{-9}$-Torr range and then rapidly fell into the $10^{-10}$-Torr range after completion of evaporation.

Energy distribution curves for Au are shown in Fig. 1 at 0.5-eV intervals for photon energies $10.2 \leq h\nu \leq 23$ eV and in Fig. 2 at 1- and 2-eV intervals for $23 \leq h\nu \leq 40$ eV. The data have been plotted to show the two-dimensional nature of the emission intensity $N(E_i, h\nu)$, where $E_i$ and $h\nu$ are the initial electron and photon energies, respectively. For $h\nu \gtrsim 15$ eV, the full width of the $d$ bands is observed. The $d$ bands are about 5.7 eV wide and extend from $-2$ to $-7.7$ eV, in agreement with earlier measurements.[4] Much structure is observed; e.g., for $h\nu = 15$ eV, $d$-band structure is seen at $-2.6$, $-3.1$, $-3.4$, $-5.1$, $-5.6$, $-6.4$, and $-6.8$ eV. The data show changes in structure (both in energy positions and amplitudes) as the photon energy is varied over the entire range of energies up to 40 eV, thus indicating that momentum conservation influences the spectra in this entire energy range. The EDC's have not converged to the x-ray photoelectron spectrum (XPS) for Au by 40 eV,[9] although the overall shapes of the EDC's in Fig. 2 (with a pronounced minimum near $-5$ eV) show a qualitative resemblance to the XPS spectrum.

The data in Figs. 1 and 2 were taken with the

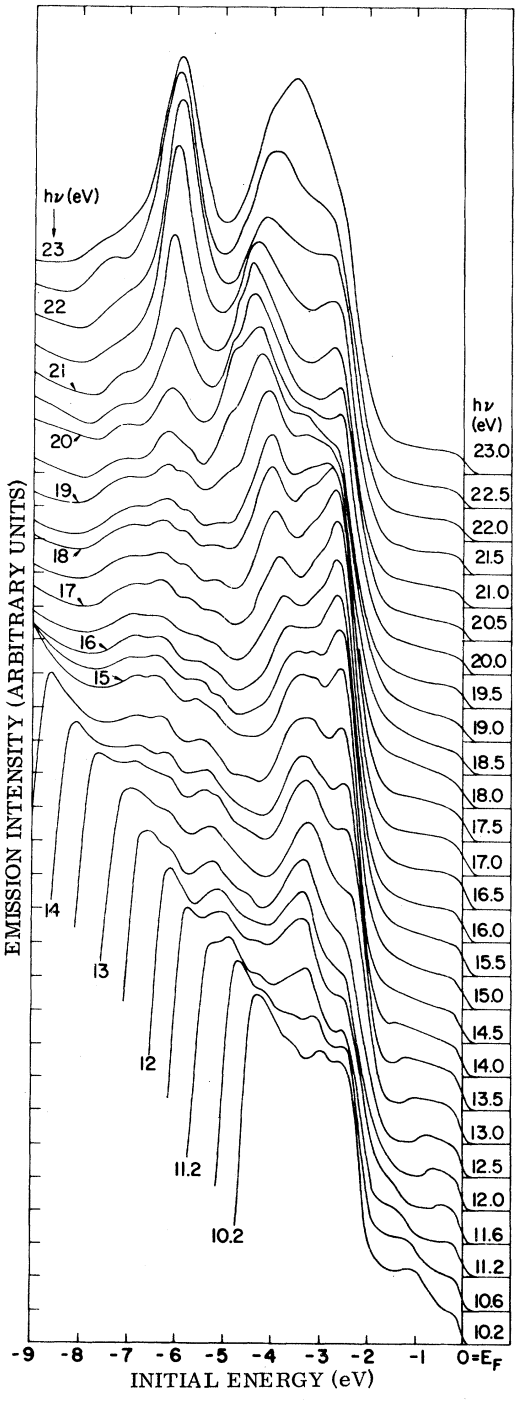


FIG. 1. Energy distributions for Au with $10.2 \leq h\nu \leq 23$ eV. The zero of energy corresponds to the Fermi level.

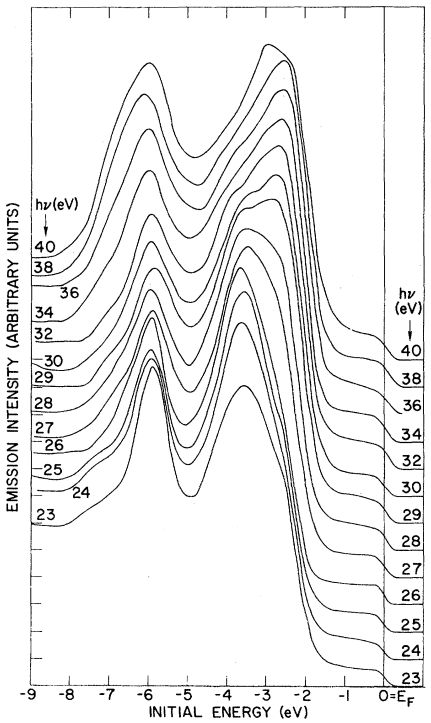


FIG. 2. Energy distributions for Au with $23 \leq h\nu \leq 40$ eV.

electron analyzer set at a 15-eV pass energy (energy resolution of $\Delta E \sim 0.12$ eV) for $h\nu \lesssim 27$ eV and set at a 25-eV pass energy ($\Delta E \simeq 0.16$ eV) for $28 \leq h\nu \leq 40$ eV. The monochromator band pass was set at $\Delta\lambda = 8$ Å for $10 \leq h\nu \leq 16$ eV, at $\Delta\lambda = 4$ Å for $16 \leq h\nu \leq 19$ eV, at $\Delta\lambda = 2$ Å for $19.5 \leq h\nu \leq 22.5$ eV, and at $\Delta\lambda = 4$ Å for $23 \leq h\nu \leq 40$ eV. Thus the total resolution was $\lesssim 0.2$ eV for $h\nu < 23$ eV and diminished to $\sim 0.3$ eV at $h\nu = 30$ eV and to 0.5 eV at $h\nu = 40$ eV. For a typical storage-ring beam current of 3 mA, signal levels for the electron analyzer were about $10^5$ counts/sec for $10 \lesssim h\nu \lesssim 15$ eV, about $2\times10^4$ counts/sec at $h\nu = 20$ eV, and about $2\times10^2$ counts/sec at $h\nu = 40$ eV.

For $10.2 \leq h\nu \lesssim 14$ eV in Fig. 1, two pieces of structure are seen in the $s$-$p$ band emission within 2 eV of $E_F$. One is a high-energy shoulder which shifts to lower energies from about $-0.8$ eV at $h\nu = 10.2$ eV to about $-1.6$ eV at $h\nu = 11.6$ eV.[11] This structure has been previously observed[5,6] and is associated with the disappearance of transitions into the lowest conduction band. For $11.6 \leq h\nu \leq 14$ eV, new $s$-$p$ band emission near $E_F$ with a boxlike shape is observed and is seen to increase in width from $\sim 0.6$ eV at $h\nu = 11.6$ eV to about 1.6 eV at $h\nu = 14$ eV. We associate this structure with $s$-$p$ interband transitions due to the $X$ (100) Bragg plane, i.e., transitions between conduction bands in the $\Gamma$-$X$ (100) direction.

The availability of photemission data over such a wide photon energy range has encouraged us to perform an average of the data over all available photon energies using a modified version of the $f$-sum rule[12] for the purpose of obtaining an experimental $d$-band density of states. The basic idea is that a given initial state can undergo transitions into a number of final states determined by the selection rules of conservation of photon energy and crystal momentum. When photoemission EDC's are averaged over the photon energy range which contributes to the optical sum rule,[13] details of the final states and transition-probability effects are largely eliminated, and a replica of the density of occupied $d$-band states should result.

We have averaged the EDC's for Au in Figs. 1 and 2 according to this idea (to be described in a later paper). The optical constants for Au due to Beaglehole[14] were used to weight EDC's according to the optical sum rule.[13] In performing the average, we eliminated threshold effects and the above-mentioned extra spectrometer emission for EDC's with $h\nu \lesssim 15$ eV by smoothly continuing the curves to $-9$ eV with an overall shape similar to those observed at higher energies and without introducing any new structure.

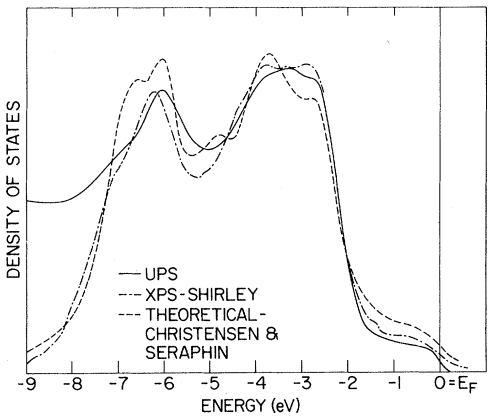


FIG. 3. Density-of-states curves for Au (see text).

Our averaged "density of states" $\bar{N}(E_i)$ determined for Au in the above-mentioned manner is shown in Fig. 3 (solid line), together with the XPS optical density of states for Au due to Shirley[9,15] and a theoretical band density of states calculated by Christensen and Seraphin[7] which was convolved with a 0.6-eV wide Lorentzian lifetime broadening function. Secondary and primary emission were not separated in performing the average of the EDC's in Figs. 1 and 2; subtraction of secondary emission would lower the amplitude of structure in $\bar{N}(E_i)$ near $-6$ eV by about $\frac{1}{3}$.

Comparison of the three curves in Fig. 3 shows good agreement of several main features, including the overall width ($\sim 5.7$ eV) and position of the $d$ bands, the large square-edged $d$-band density of states extending from about $-2$ to $-4.5$ eV, the minimum near $-5.25$ eV, and the sharp peak near $-6$ eV with a shoulder at lower energy (near $-6.5$ to $-7$ eV).

In comparing XPS and the above-described UPS methods of determining $d$-band densities of states, several comments can be made. An advantage of XPS is its comparative experimental simplicity. Potential advantages of the UPS method are (1) better resolution (e.g., see Fermi-level edges in Fig. 3), and (2) relative transition-probability effects for different $d$-band states should be eliminated. The latter is nullified to some extent by the effects of secondary electron emission (which is more difficult to separate at low photon energies), and by threshold cutoff effects.

We gratefully acknowledge the able assistance and cooperation of the members of the storage

ring group at the Physical Sciences Laboratory.

*Work supported in part by the U. S. Air Force Office of Scientific Research under Contracts No. F44620-70-0089 and No. F44620-70-C-0029.

[1]C. Gahwiller *et al.*, Rev. Sci. Instrum. 41, 1275 (1970).

[2]D. Blechschmidt *et al.*, Opt. Commun. 1, 275 (1970).

[3]Y. Iguchi *et al.*, Phys. Rev. Lett. 26, 82 (1971).

[4]D. E. Eastman and J. K. Cashion, Phys. Rev. Lett. 24, 310 (1970).

[5]W. F. Krolikowski and W. E. Spicer, Phys. Rev. B 1, 478 (1970).

[6]N. V. Smith, Phys. Rev. B 3, 1862 (1971), and in *Electron Spectroscopy*, edited by D. A. Shirley (North-Holland, Amsterdam, 1972).

[7]N. E. Christensen and B. O. Seraphin, Phys. Rev. B 4, 3321 (1971).

[8]A. R. Williams, J. F. Janak, and V. L. Moruzzi, Phys. Rev. Lett. 28, 671 (1972).

[9]D. A. Shirley, in *Electron Spectroscopy*, edited by D. A. Shirley (North-Holland, Amsterdam, 1972).

[10]S. Z. Sar-El, Rev. Sci. Instrum. 38, 1210 (1969).

[11]For low photon energies ($\lesssim 15$ eV) in Fig. 1 we observe extra emission ($\lesssim 20\%$ for $h\nu \leq 11.6$ eV) due to stray light and/or secondary electron emission which results in the lowest energy peak at the left of each EDC but does not introduce any additiona structure.

[12]F. Seitz, *The Modern Theory of Solids* (McGraw-Hill, New York, 1970), p. 650.

[13]H. Ehrenreich and H. R. Philipp, Phys. Rev. 128, 1622 (1962).

[14]D. Beaglehole, Proc. Phys. Soc., London 85, 1007 (1965).

[15]We have shifted Shirley's XPS spectra upwards in energy by 0.15 eV in order to better match our $d$-band edge.

# Band-Structure Calculation of the Electron Spin Polarization in Field Emission from Ferromagnetic Nickel*

Beverly A. Politzer

*Department of Physics, The Pennsylvania State University, University Park, Pennsylvania 16802*

and

P. H. Cutler†

*Surface Physics Division, European Space Research and Technology Organization, Noordwijk, Holland*

(Received 7 February 1972)

A detailed $3d$ band structure of ferromagnetic Ni is incorporated into a calculation of the electron spin polarization in field emission from the (100) crystal plane. In agreement with a recent experiment of Gleich, Regenfus, and Sizmann, the calculated electron spin polarization is found to $-4\%$, with the preferred spin direction parallel to the magnetization of the crystal.

Several recent measurements of electron spin polarization (ESP) in photoemission[1,2] and field emission[3] from Ni have produced controversy concerning the validity of the Stoner-Wolfarth-Slater (SWS) itinerant band model of ferromagnetism.[1-5] The following Letter describes the first application of a detailed SWS band structure in a rigorous calculation of the ESP in field emission from the (100) plane of ferromagnetic Ni. The results agree in sign and magnitude with ESP measurements of Gleich, Regenfus, and Sizman[3] for field emission around the [100] crystallographic direction of Ni.

The essential features of the model employed in the calculation are as follows: The emission or "$z$" direction coincides with the [001] direction of a semi-infinite fcc crystal of Ni. The emission surface at $z=0$ is $\frac{1}{2}a$ away from the last atom layer present, where $a=3.5$ Å is the interatomic spacing for fcc Ni. It is assumed the emission plane exhibits the two-dimensional translational symmetry of a (100) plane of the infinite lattice, and hence the condition for specular reflection and transmission is satisfied. The surface potential is represented by a triangular barrier given by $V(z)=-eFz$, $z>0$, with $F$ denoting the applied electric field. The SWS itinerant band model is invoked to account for the ferromagnetic properties of Ni. Specifically, the unhybridized $3d$ and $4s$-$p$ conduction bands are divided into identical spin bands, majority ($\uparrow$) and minority ($\downarrow$), separated by the exchange energies $\Delta E_{\mathrm{exch}}{}^{(d)}=0.03$ Ry and $\Delta E_{\mathrm{exch}}{}^{(s)}=0$. The $4s$-$p$ spin bands are approximated by parabolic free-electron bands originating at $\Gamma_0$. The $3d$ bands are described by a tight-binding calcula-